Hindawi
Advances in Tribology
Volume 2019, Article ID 4981246, 15 pages
https://doi.org/10.1155/2019/4981246

Research Article

High Temperature Friction and Wear Performance of PVD Coatings under Press Hardening Contact Conditions

Sergej Mozgovoy, Jens Hardell, and Braham Prakash

Division of Machine Elements, Luleå University of Technology, 971 87 Luleå, Sweden

Correspondence should be addressed to Sergej Mozgovoy; sergej.mozgovoy@ltu.se

Received 9 November 2018; Revised 8 March 2019; Accepted 18 March 2019; Published 17 April 2019

Academic Editor: Huseyin Çimenoğlu

Press hardening is widely employed to produce automotive structural and safety components from advanced high-strength steels. This process depends on friction between the forming tools and the work piece. Wear of the forming tools affects the dimensional accuracy of produced components and reduces their service life. It is therefore desirable to reduce wear of forming tools for press hardening applications. One way to achieve this is by applying hard physical vapour deposited (PVD) coatings on the tool. In this work, the tribological behaviour of PVD coated tool-work piece material pairs has been studied at elevated temperatures in an experimental set-up simulating the tribological conditions in press hardening. Four different PVD coatings deposited on tool steel and uncoated tools as reference were studied during sliding against uncoated and Al-Si coated 22MnB5 steel. Results show that uncoated tools exhibited the lowest coefficient of friction when sliding against uncoated 22MnB5 steel. A CrWN coating initially showed low coefficient of friction but it increased with increasing sliding distance. A TiAlN coating and one of two AlCrN coatings showed similar frictional behaviour when sliding against uncoated 22MnB5 steel. During sliding against uncoated 22MnB5 steel, adhesive wear has been found to be the dominant wear mechanism. Adhesive wear was considerably reduced in the case of hard PVD coated tools in comparison to that of uncoated tools. During sliding against Al-Si coated 22MnB5 steel, no clear advantage in terms of friction behaviour of uncoated or PVD coated tools was observed. However, the transfer of Al-Si coating material from the work piece to the tools was significantly reduced for PVD coated tools. Frictional instabilities in all cases involving Al-Si coated work piece material further confirmed the occurrence of adhesive material transfer.

1. Introduction

Press hardening is widely employed to produce automotive structural and safety components from advanced high-strength steels. This process depends on friction between the forming tools and the work piece as it affects the dimensional accuracy of produced components. Wear of the forming tools reduces their service life and influences the process economy. Wear of the surfaces can also affect the friction during the tool and work piece interaction. It is therefore desirable to control friction as well as reducing wear of forming tools for press hardening applications. One way to achieve this is by applying hard PVD coatings on the tool. Hardell and Prakash [1] evaluated the friction and wear characteristics of plasma nitrided, CrN, and TiAlN coated tool steels under unidirectional sliding against 100Cr6 bearing steel under unlubricated conditions at room temperature and 400°C. The CrN and TiAlN coatings showed relatively high but stable friction coefficients at room temperature. Wear was negligible in the case of the CrN coating and material was transferred from the counterface to the TiAlN coating at room temperature. At 400°C, the coefficient of friction of the CrN coated tool steel was lower than at room temperature. The TiAlN coating showed very unstable and high friction coefficients owing to adhesion and transfer of the coating to the counterface. Furthermore, it was concluded that exposure of the tool coatings to elevated temperature and subsequent testing at room temperature resulted in higher friction and more wear on the counterbody. However, detailed insights into why the TiAlN coating transferred to the counterbody were not given. Wieland and Merklein [2] studied the possibility of reducing adhesive wear under complex loading conditions by applying an AlCrN monolayer coating on the tool steel and comparing its behaviour to an uncoated tool. An undesirable

increase in surface roughness on the AlCrN coated tool was observed as compared to the change in roughness of the uncoated tool. Material build-up seemed to be higher on the coated tool but the amount of transferred material was less than for the uncoated tool. However, only Al-Si coated work piece material was considered and information about friction coefficients or specific wear rates was not given. Kondratiuk and Kuhn [3] studied the tribological behaviour of multilayered TiN/TiB_2 and monolayered AlCrN tool coatings when sliding against Al-Si coated 22MnB5 at 880°C and 920°C and against Zn-Ni coated 22MnB5 at 880°C. In the case of Al-Si coated 22MnB5 steel, the friction coefficient started with a high initial value but it decreased to a steady state value with sliding distance. The coefficient of friction was also found to decrease with increasing load whereas it was independent of the load and steadily increased in the case of Zn-Ni coated 22MnB5 steel. Wear of the work piece was higher for the Zn-Ni coated sheets than for Al-Si coated ones. The performance of the AlCrN coating on the tool was reported to be better than that of the TiN/TiB_2 multilayered tool coating. Additionally, a higher blank temperature resulted in less wear when sliding against the AlCrN coated tool. The authors concluded that the wear rates of the tool coatings were generally dominated by the hardness of the worn material. Mass loss from the Zn-Ni coated work piece was higher due to formation of zinc oxide but less build-up of metallic material on the forming die was more advantageous for the press hardening process. The authors investigated friction and wear behaviours by using different experimental set-ups and it is therefore difficult to compare these obtained results pertaining to tribological characteristics. Neugebauer et al. [4] investigated CrVN, NbTiAlN, and TiZrCrN tool coatings in view of their capabilities to improve process stability in press hardening of boron-manganese-steels. These tool coatings were tested against uncoated, Al-Si coated, and Al-Si-graphite coated 22MnB5 steels. The results showed that the coefficient of friction was approximately halved in the case of Al-Si-graphite coated 22MnB5 when comparing to uncoated 22MnB5 steel. Furthermore, the authors found that adhesion of uncoated 22MnB5 on an uncoated tool led to an increase in surface roughness. The CrVN coated tool was characterised by very low roughness after sliding against the Al-Si-graphite coated 22MnB5 when compared to the other two work piece materials. The mono layered NbTiAlN and TiZrCrN exhibited lower roughness in the case of uncoated 22MnB5 steel than for Al-Si-graphite coated 22MnB5. However, specific wear rates for the coating materials were not reported and the wear mechanisms were not explained in detail. Sánchez-López et al. [5] studied the tribological behaviour of Y or Zr doped CrAlN coatings as well as doped and undoped CrAlN coatings with varying Al content at temperatures between ambient and 650°C when sliding against alumina in a ball on disk configuration. The authors found that the wear mechanism was mainly abrasive and governed by the formation of a mixture of chromium and aluminium oxides whose composition was determined by the initial chemical composition of the coating as well as the testing temperature. For CrAlN, wear was mainly abrasive whereas CrAlYN and CrAlZrN showed more adhesive wear behaviour. It was deduced that the doping of CrAlN coatings was beneficial when aluminium content in the coating was low. The addition of Zr promoted the formation of Cr_2O_3 that resulted in lower and stable friction and decreased wear of the counter-surface. The addition of Y up to 2 at.% resulted in reduced wear of the coating up to 500°C but had no effect at higher temperatures. Furthermore, when the Al content in the coating increased, the friction coefficient increased, but wear of the coating decreased due to a higher hardness of the coating and the presence of aluminium oxides on the coating surface. However, the formation of Al_2O_3 on the coating surface resulted in more wear of the counter-surface.

This brief overview shows that the friction and wear performance of hard PVD tool coatings for use in press hardening applications have not been studied in detail. The motivation for conducting the present study is mainly in view of evaluating hard PVD coatings under contact conditions prevalent in the press hardening process regarding their tribological performance. In a previous work, we investigated the influence of sliding velocity, normal load, and work piece surface material (uncoated or Al-Si coated 22MnB5 steel) on the tribological behaviour of plain quenched and tempered tool steel [6]. The mechanisms behind material transfer occurring at elevated temperatures need to be fully understood in order to develop strategies to prevent material transfer from the work piece to the forming tool. Hence, the tribological behaviour of PVD coated tool-work piece material pairs at elevated temperatures has been studied in an experimental set-up simulating the tribological interaction between tool and work piece in press hardening. The long-term aim is to understand in detail the mechanisms of friction and wear at elevated temperatures in order to develop ways to prolong the tools' service life.

2. Experimental Work

In this work, we followed the experimental methods described in detail by Mozgovoy et al. (2017) in [6]. This section gives an overview of the used materials and specimen geometries as well as the employed experimental equipment and followed test procedure.

2.1. Test Materials and Specimens. In this study, the base materials and specimen geometries were the same as employed by Mozgovoy et al. (2017) [6]. The chemical compositions of the different materials used in the current work are summarised in Table 1. Tribological experiments were performed on a prehardened hot work (quenched and tempered) tool steel with and without surface modifications. The microstructure of the tool steel specimens consisted of tempered martensite. These tool steel specimens were cuboidal specimens with a width of 10 mm, a depth of 10 mm, and a height of 20 mm. The contact surface of tool steel specimens was machined with a double radius of 50 mm resulting in a spherical tip. The spherical contact surfaces were finely ground with grit size P600 silicon carbide grinding paper to achieve a predeposition surface roughness R_a of $0.13 \pm 0.01\ \mu$m. The point contact generated by the spherical tip against the flat counter surface was employed to

Table 1: Alloying composition in wt.% (Fe makes up the balance), initial hardness, and surface roughness of investigated sheet and tool steel materials (values in parenthesis are for Al-Si coated 22MnB5).

Material	C	Si	Mn	P	S	Cr	Mo	V	Ni	B	$HV_{0.5}$	R_a (μm)	Comments
22MnB5	0.20 – 0.25	0.20 – 0.35	1.0 – 1.3	max. 0.03	max. 0.01	0.14 – 0.26	–	–	–	0.005	201 ± 3	1.16 (0.90) ± 0.16 (0.18)	as delivered
Tool steel	0.32	0.6 – 1.1	0.8	max. 0.01	max. 0.003	1.35	0.8	0.14	max. 1	–	458 ± 6	0.13 ± 0.01	prior to coating

Table 2: Thickness, initial surface roughness, and hardness of the investigated PVD coatings.

Material	Thickness (μm)	Roughness R_a (nm)	Hardness $HV_{0.05}$	Plasma nitrided substrate
TiAlN	3.8 ± 0.1	104 ± 19	1599 ± 59	Yes
AlCrN 1	2.7 ± 0.2	128 ± 27	1006 ± 54	Yes
CrWN	4.4 ± 0.3	83 ± 20	1214 ± 51	No
AlCrN 2	7.2 ± 0.1	158 ± 26	2316 ± 168	No

simulate severe contact conditions, e.g., on a die radius. In the current work, four different coatings were deposited on the contact surface of the tool steel specimens through physical vapour deposition (PVD). Uncoated tool steel specimens were used as a reference. TiAlN and AlCrN 1 coated tool steel specimens were plasma nitrided prior to coating deposition whereas plasma nitriding of the tool steel substrate was omitted on CrWN and AlCrN 2 coated tool steel specimens. After deposition, the coatings were polished with liquid diamond suspension containing particles of 1 μm size to remove residual surface irregularities, e.g. droplets, on the hard coatings generated during the deposition process. In Table 2, thickness as well as surface roughness (postpolished) and hardness of the investigated PVD coatings are summarised. It should be noted that the reported hardness values are the system's hardness including coating and substrate and that surface roughness and hardness values were averaged from a total of five measurements. The surface roughness R_a of the postpolished PVD coatings before tribological testing averaged out at 0.12 ± 0.03 μm. The studied work piece materials were as-delivered uncoated and Al-Si coated 22MnB5 steels. The work piece specimens were cut from actual sheets with a thickness of 1.5 mm to a width of 15 mm and a length of 1000 mm. These 22MnB5 steel strips initially had a ferritic-pearlitic microstructure and were used in their as-delivered surface condition.

2.2. Test Equipment. For high-temperature friction and wear studies, the hot strip tribometer described in more detail by Mozgovoy et al. (2017) in [6] was used to investigate the tribological characteristics of hard coated tool-22MnB5 work piece strip material pairs. The custom-built hot strip tribometer consists of hydraulically actuated clamping jaws that secure the work piece strip. An electric motor drives a tool assembly through a ball screw to slide two tool pin specimens along the work piece strip. A pneumatic cylinder applies a pretension force to one of the clamping jaws in order to keep the work piece strip straight during experimentation. Two specimen holders for the tool pin specimens are installed in the movable tool assembly together with different sensors. Figure 1 illustrates the top view of this basic configuration of the test equipment. A pneumatic bellow loads the movable tool pin specimen (top in Figure 1) against the work piece strip and the stationary tool pin specimen (bottom in Figure 1). The two tool pin specimens are then slid along the length of the work piece strip. During sliding, the tangential forces occurring and the applied normal force are measured by strain gauge force transducers. The coefficient of friction is then calculated according to following equation:

$$\mu = \frac{F_F - F_P}{2F_N} \tag{1}$$

where F_F is the friction force, F_P is the pretension force, and F_N is the applied normal force as shown in Figure 1.

Under the tribometer assembly, new work piece strips are automatically fed from a stacking tray into the clamping jaws and worn work piece strips are automatically put back into the tray. In this way, accelerated wear on the tool pin specimens can be induced. In addition, the use of individual work piece strips allows understanding changes in friction and wear mechanisms with respect to their position on the work piece strip. Accumulation of wear debris is limited as the work piece strip is mounted vertically during experimentation. Above mentioned clamping jaws also provide the resistive heating of the work piece strip. The temperature of the work piece strip is continuously measured by a pyrometer in front of the tool assembly. The temperatures of the tool pin specimens are measured about 5 millimetres from the contact interface by means of type-k thermocouples. In the current study, the work piece strip was not quenched after testing as the intention was to investigate the sliding motion of the forming step under severe contact conditions. During experiments, a LabView®-based data acquisition and control software monitors and measures normal force, sliding (friction) force, pretension force, specimen temperatures, and strip current.

2.3. Test Procedure. The experimental method described in [6] by Mozgovoy et al. (2017) was followed in this work. First, the tool pin specimens were cleaned in an ultrasonic cleaner

Table 3: Test parameters used in high-temperature tribological tests.

Test parameter	Load in N	Velocity in $m \cdot s^{-1}$	Strip temperature in °C	Initial tool temperature in °C	Sliding distance per strip in m	Atmosphere (1 atm)
Value	150	0.1	750	25	0.55	air

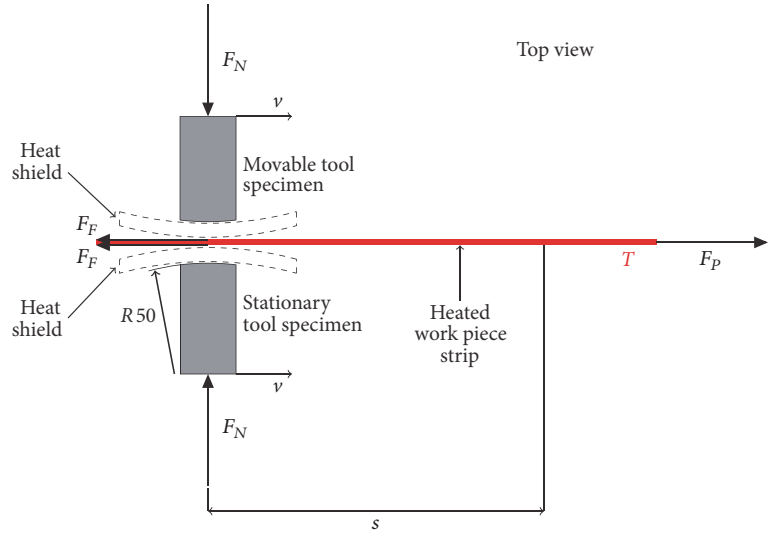

Figure 1: Top view schematic showing hot strip tribometer experimental configuration employed in tribological studies; F_N is the normal force, F_F is the friction force, F_P is the pretension force, T is the temperature of the work piece, v is the velocity and s is the sliding distance per work piece strip. Note that positions of heat shields during heating are indicated and that specimens are not according to scale.

in heptane and in ethanol. Each specimen was weighed five times in a semimicro analytical laboratory balance before averaging its mass. Then, the tool pin specimens were mounted in separate specimen holders and installed in the tribometers tool assembly. Type K thermocouples were inserted in the tool pin specimens from the back to measure the temperature about 5 mm from the contact surface. Alumina heat shields were put between the tool specimens and the work piece strip to avoid their adherence during heating. The work piece strip specimens were wiped clean with heptane and ethanol. A total of ten work piece strips were used in one experiment. This adds up to a total sliding distance of 5.5 m, which generates measurable wear on the tool pin specimens. The test parameters specified in Table 3 were employed during experimentation.

In the current work, a work piece temperature of 750°C for uncoated and Al-Si coated strips was employed as it represents a temperature relevant for press hardening. In case of uncoated 22MnB5 strips, the strip heating was executed by the software by setting the parameters of the PID controller. As the work piece strip is heated in air, the uncoated 22MnB5 steel will be susceptible to oxidation, decarburization, and scaling during heating and tribological testing. Therefore, the heating time was limited to 180 s to prevent excessive growth of the oxide layer. In the case of Al-Si coated 22MnB5 work piece strips, the strip heating was manually controlled by setting the power input to reproduce the stratified morphology of the coating. A total duration of approximately seven minutes consisting of three different power input steps (temperatures) and holding times (diffusion kinetics) resulted in a morphology of the coating similar to what is observed in press hardening. The work piece strip reached its austenitisation temperature of 920°C during this heat treatment before the power input was reduced to reach the test temperature of 750°C.

The ceramic heat shields were removed when the desired test temperature was attained. Then, the normal load was applied and when it stabilised (error margin of ±1.4% determined after tests), the tribological experiment was carried out. As mentioned above, ten work piece strips were tested in each experiment. Moreover, each experiment was also performed twice. After the test, the tool pin specimens were removed and cleaned in an ultrasonic cleaner in ethanol. The worn pin specimens were also weighed five times in order to determine their average weight change. The obtained weight change was converted to volume by utilising the density of steel (7.85 g/cm^3) as a first approximation. Depending on which phases are transferred to the tool surface, in general, the density of any material transfer film is a combination of their varying densities, e.g., Fe_2Al_5 possesses a density of 7.9 g/cm^3 whereas $FeAl_2$ exhibits a density of 4.18 g/cm^3 according to [7]. As the Al-Si coating consists of a stratified morphology, the density of steel was employed for relative comparison. Though, the largest volume of the Al-Si coating consists of the two binary intermetallic phases Fe_2Al_5 and

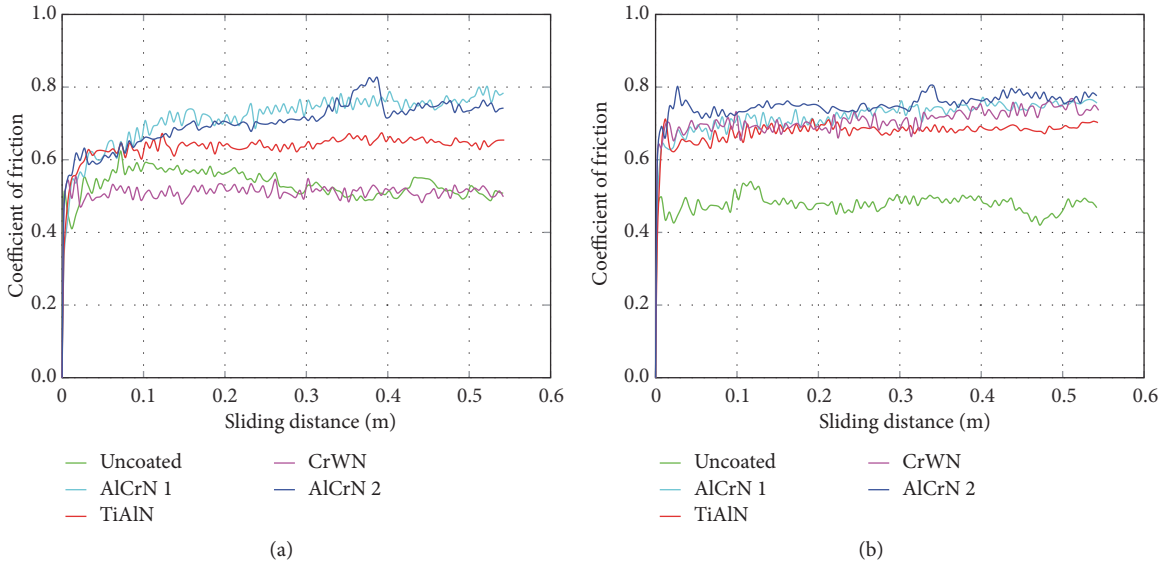

Figure 2: Coefficient of friction as a function of sliding distance for (a) 1st and (b) 10th uncoated 22MnB5 steel strip.

$FeAl_2$. Average specific wear rates were deduced from the determined volumes as per

$$k = \frac{V}{F_N \cdot s} \tag{2}$$

where k is the specific wear rate as reported by Archard, V designates the volume worn away (mm^3), F_N is the normal load (N), and s denominates the total sliding distance (m) [8, 9].

2.4. Analysis. A Veeco Wyko NT 1100 optical interferometer was employed to measure the initial surface roughness R_a. The hardness was measured with a Matsuzawa MXT-α microhardness tester using a load of 0.5 kg for bulk hardness and a load of 0.05 kg for coating hardness. A Jeol JSM-IT300 environmental scanning electron microscope (SEM) in conjunction with energy-dispersive X-ray spectroscopy (EDX) was employed in secondary electron mode or in combined backscattered electron mode to evaluate the surface morphology and friction and wear mechanisms of specimens by using 15 or 20 kV accelerating voltage and working distances between 10 and 12 mm. X-ray diffraction (XRD) performed in a PANalytical Empyrean diffractometer was employed to identify the phases present on tool specimens that were subjected to material transfer after contact with Al-Si coated 22MnB5 sheet strips.

3. Results and Discussion

In this section, the results pertaining to friction and wear experiments and analyses of the worn specimens are presented and discussed. The findings and observations are first given for uncoated 22MnB5 sheet steel and then for Al-Si coated sheet material as this part of the tribological system mainly governs the tribological behaviour. Since Al-Si coated 22MnB5 steel is more readily used in press hardening and the severity of material transfer (galling) is more pronounced, more focus is given to the analysis of the results regarding Al-Si coated 22MnB5 sheet steel in this work.

3.1. Tools Sliding against Uncoated 22MnB5 Steel. The friction behaviour for the first and tenth strip of four different PVD tool coatings and uncoated tools during sliding against uncoated 22MnB5 steel at 750°C is shown in Figure 2. The uncoated tool steel exhibited the lowest coefficient of friction. CrWN coated tool steel initially showed low coefficient of friction but it increased with increasing sliding distance. TiAlN coated tool steel and the two AlCrN coated tool steels did not differ significantly in their frictional behavior when sliding against uncoated 22MnB5 steel. For these three PVD coatings, the coefficient of friction was unstable and the steady state level varied between individual sheet strips. No significant difference in frictional performance due to plasma nitriding of the AlCrN 1 coated tool steel sliding against uncoated 22MnB5 can be observed when comparing to the AlCrN 2 coated tool steel without plasma nitriding. Very unstable and high friction coefficients were reported by Hardell and Prakash for TiAlN coated tool steel sliding against 100Cr6 bearing steel at 400°C [1]. As the tool pins initially are at room temperature, apart from a running-in phase, a comparable instability in the coefficient of friction of TiAlN coated tool steels and even AlCrN coated tool steels sliding against uncoated 22MnB5 steel at 750°C is observed in this work.

Figure 3 depicts the specific wear rates for uncoated and PVD coated tools sliding against uncoated 22MnB5 steel. It can be observed that the specific wear rates of PVD coated tools are less than a quarter compared to the uncoated reference tool. Similar observations were reported by Neugebauer et al. [4]. Furthermore, if a comparison between the wear behaviours of the different PVD coatings

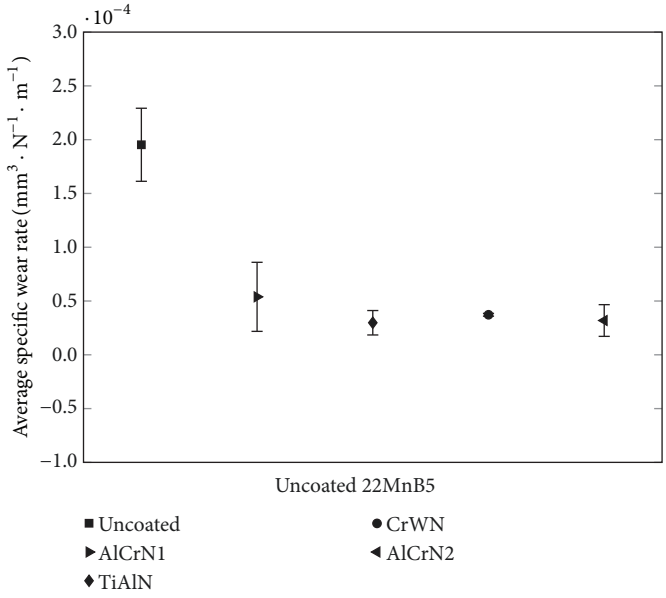

Figure 3: Average specific wear rate of uncoated and PVD coated tool steels sliding against uncoated 22MnB5 steel.

is made, it can be seen that the average specific wear rate of a thinner PVD coating increases when sliding against uncoated 22MnB5 steel.

3.1.1. Characteristics of Uncoated Tool Steel. In the initial point contact, the mean Hertzian contact pressures at 150 N normal load and 750°C corresponded to about 270 MPa for uncoated tools and about 290 MPa for PVD coated tools. An apparent flat circular contact area of approximately 1.5 mm radius was observed on uncoated and PVD coated tools after testing. Hence, the contact pressures should be reduced to about 21 MPa at the end of tribological tests. Such contact pressures, even though they are estimated, lead to local plastic deformation and flattening of surface asperities. It was observed in Figure 2 that uncoated tool steel pins sliding against uncoated 22MnB5 steel exhibited the lowest coefficient of friction. One explanation for this behaviour is that the indentation depth of uncoated and PVD coated tools according to Hertzian theory is initially almost identical, but uncoated tool steel is softer and will be subjected to more wear. This leads to a faster reduction in contact pressure and a reduced coefficient of friction compared to PVD coated tools, which will have a larger contribution from ploughing friction. In Figure 4, a brindled pattern of light and dark grey areas on the uncoated tool pin surface tested against uncoated 22MnB5 steel can be identified. Energy-dispersive spectra taken at positions (1) and (2) as indicated in the micrograph revealed that these two areas contained different amounts of oxygen. The rapid Joule heating of the uncoated 22MnB5 steel strip in air limits the amount of static oxidation before reaching the testing temperature of 750°C. As explained in [6], the strip surface can therefore be assumed to be in a transient stage of oxidation which influences the tribological behaviour during sliding. As stated by Stott and Wood [10], oxide in a transient stage of oxidation is removed by the sliding action as the cohesion of the oxide to its native metal is weak. The worn tool surface consists of metallic material (light grey) that also is in a momentary state of oxidation due to the heat transfer between tool pin and sheet strip, as indicated by the smaller oxygen peak in spectrum (1) in Figure 4. Moreover, the worn tool surface is also comprised of oxide (dark grey) as shown by the large oxygen peak in spectrum (2) in Figure 4. As numerical simulations of the press hardening process have shown that the tool temperature seldom exceeds 400°C and no weight gain due to oxidation has been observed for the uncoated tool material in previous static experiments up to these temperatures, it is very likely that the oxide on the worn tool surface is agglomerated and compacted oxidised wear debris rather than oxide scale [11, 12].

The formation of adhesive junctions between asperities during sliding is evident from the irregular features on the worn surfaces associated with adhesive wear. As transient oxide is removed by the sliding action, many newly formed asperities are metallic in nature and, thus, the growth of adhesive junctions is significant and the high temperature will also facilitate the formation of atomic bonds. Hence, considerable metal-to-metal contact occurs which results in relatively high coefficients of friction and substantial wear. If some asperities are ceramic in nature (oxidised), growth of adhesive junctions still might occur due to the transient stage of oxidation of the surfaces and the high temperature in the contact. Archard and Hirst stated that the extent of deformation of touching surface asperities (but also their removal in this work) under the applied load determines the real area of contact [8]. This results in a growth of contact area until, according to Stott and Wood [10], the pressure in the asperity contacts drops to such an extent that the growth of adhesive junctions ends. This, however, leads to a reduced coefficient of friction and reduced wear. In the zones

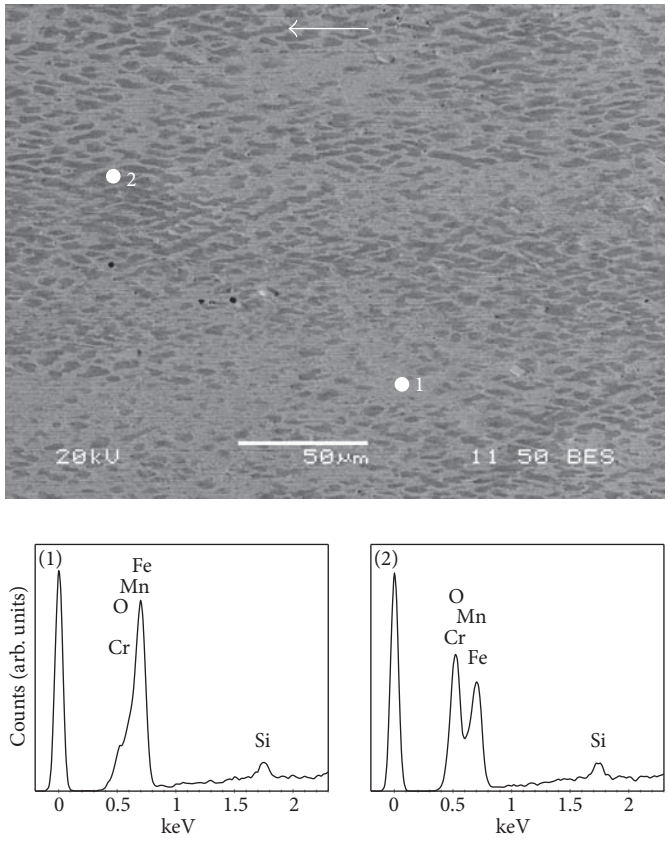

Figure 4: Scanning electron micrograph in backscatter mode of uncoated tool steel tested against uncoated 22MnB5 steel and energy-dispersive spectra taken at positions (1) and (2) in the micrograph; arrow indicates the sliding direction.

of metallic adhesive junctions on the surface (cf. light grey areas), the material from the tool surface will be displaced relatively to its initial position where the junction appeared (smearing) as the adhesion is strong while brittle failure of oxidised junctions occurs (cf. dark grey areas), which results in the brindled pattern observed on the uncoated tool steel pin surfaces in Figure 4.

3.1.2. Characteristics of PVD Coated Tool Steel. Figure 5(a) shows as an example the abrasive wear in the form of smoothing and polishing of the AlCrN 2 coating during sliding against uncoated 22MnB5 steel. Accumulation of debris and smearing of transferred material at the entrance of the contact occurs where the gap between the tool and sheet surfaces becomes smaller. This means that on a radius, debris will get entrapped through mechanical locking just in front of the contact due to the geometrical shape of the tool specimens. The TiAlN coated tool pins showed a similar behaviour. However, the CrWN and AlCrN 1 coatings did not show the accumulation of debris and adhesive smearing at the entrance of the contact even though these specimens showed polished contact zones and could also be worn through. Nevertheless, Figure 5(b) shows a material transfer layer on a CrWN coated tool pin that slid against uncoated 22MnB5 steel. Element mapping revealed that this transfer layer mainly contained Fe and O, which indicates that the material originated from the counter surface. As previously mentioned, the strip surface is assumed to be in a transient stage of oxidation and that oxides in such a state are removed by the sliding action as the cohesion of the oxide to its native metal is weak. Then, the transferred material on the CrWN coating is agglomerated and compacted oxidised 22MnB5 sheet material debris that adheres to the PVD coated surface. Figure 5(c) shows the contact zone of an AlCrN 2 coated tool pin at higher magnification. It can be observed that in the smooth contact area of the PVD coating, a considerable amount of defects or imperfections have appeared or are still present despite the polishing process of abrasive wear particles. A significant area in this smoothed contact zone has already been covered through the adhesion of debris, its accumulation, fragmentation, compaction, and oxidation as well as mixing with metallic particles.

It appears that sites where adhesion is observed, even for specimens where debris accumulates in the converging gap, are random but at the location of a defect or imperfection in the surface. There are even zones in the polished areas where no adhesive wear on the coating occurred. This suggests that the main mechanism for the occurrence of adhesion is direct adhesion followed by agglomeration and compaction of generated debris. Pelcastre et al. [13] observed a comparable mechanism of direct adhesion between PVD coated tool steel specimens and Al-Si coated 22MnB5 steel.

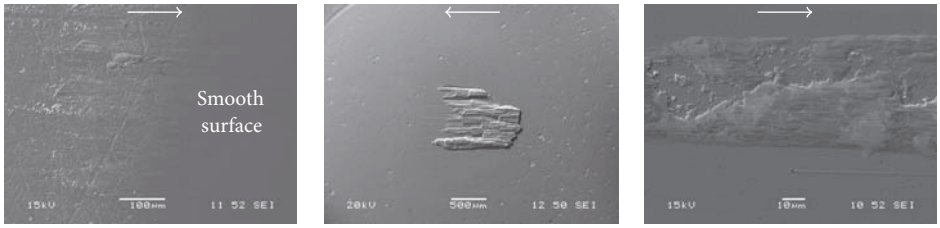

Figure 5: Scanning electron micrographs in secondary mode of (a) an AlCrN 2 coated tool pin and (b) a CrWN coated tool pin as well as (c) an AlCrN 2 coated tool pin at higher magnification after sliding against uncoated 22MnB5 steel; arrows indicate the sliding direction.

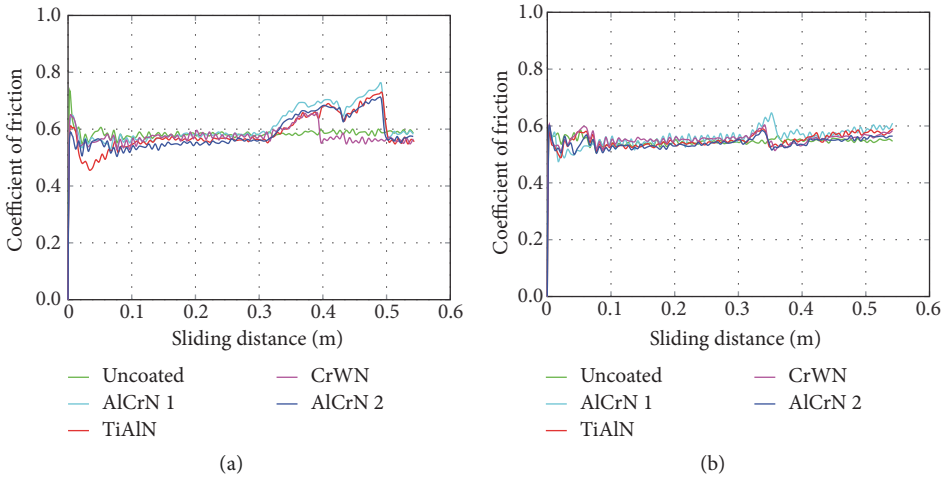

Figure 6: Coefficient of friction as a function of sliding distance for (a) 1st and (b) 10th Al-Si coated 22MnB5 steel strip.

One explanation for the occurrence of severe direct adhesion could be a chemical affinity between the PVD coatings and the transient oxide scale on uncoated 22MnB5 steel. However, a vital difference in the mechanisms between uncoated tools and PVD coated tools sliding against uncoated 22MnB5 steel does not seem to exist. Adhesive junctions seem to form in both cases, but the bonding is formed between different chemical species, Fe-Fe bonds for the former, and Fe-Coating constituents for the latter. Though, the severity of direct adhesion is more important for the formation of Fe-Fe bonds as the average specific wear rate for tool steel sliding against uncoated 22MnB5 steel in Figure 7 was higher compared to PVD coated tool steel. Once the PVD coatings are worn through, the wear mechanisms of PVD coated tool pins essentially transform into the ones observed on uncoated tools (except for the generation of coating debris). However, the affected area is smaller for the PVD coated tool steel than for uncoated tool steel, at least until the observed stages of sliding up to ten consecutively tested sheet strips. Nonetheless, the PVD coatings fail to protect the tool steel from material removal or transfer.

3.2. Tools Sliding against Al-Si Coated 22MnB5 Steel. The friction behaviour for the first and tenth strip of four different PVD tool coatings and uncoated tools during sliding against Al-Si coated 22MnB5 steel at 750°C is given in Figure 6. It is revealed that the friction behaviour of uncoated and PVD coated tools is indistinguishable during sliding against Al-Si coated 22MnB5 steel. After the transition from static to dynamic friction during the first 0.1 m of sliding on the first sheet strip, friction stabilises at the same steady state value for all successively tested sheet strips. A similar behaviour was observed by Kondratiuk and Kuhn [3]. After running-in of the tool surfaces during the first 0.1 to 0.2 m of sliding on the first sheet strip, a sudden increase in the coefficient of friction after 0.3 m of sliding on each tested sheet strip is observed. The sliding distance along which the friction coefficient is high and unstable after its increase only differs for the first sheet strip. Later, the increase in coefficient of friction occurs approximately for the same length for any tool pin pair on all consecutively tested sheet strips. This very similar friction behaviour for the tool materials during sliding against Al-Si coated 22MnB5 steel suggests that friction is governed by the Al-Si coating on the 22MnB5 sheet material whereas the tool coating does not influence the friction behaviour significantly. Such a frictional response was also observed by others [4, 14]. Furthermore, plasma nitriding prior to deposition of the coatings does not influence the friction behaviour.

Figure 7 shows the specific wear rates for uncoated and PVD coated tools sliding against Al-Si coated 22MnB5 steel. It can be observed that the transfer of Al-Si coating material

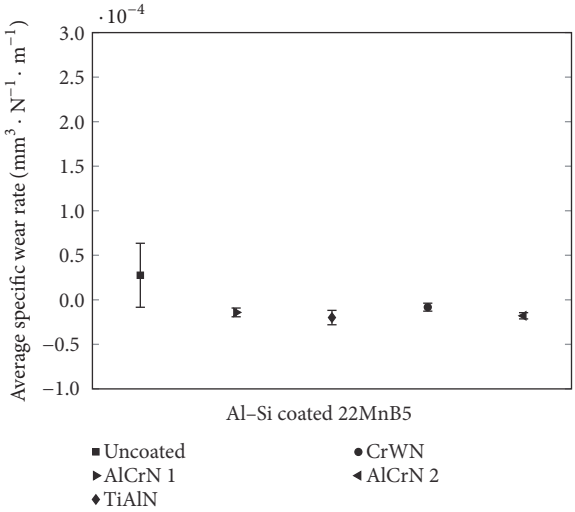

Figure 7: Average specific wear rate of uncoated and PVD coated tool steel sliding against Al-Si coated 22MnB5 steel.

from the work piece to the tools does not result in material removal from the tool surface in the case of PVD coated tools. Similar observations for various PVD nitride coated tools were reported by others [2–4]. These findings suggest that the build-up of transferred material on surface engineered tools can be less severe when adhesive bonds to these tools are not as readily formed. In this study, both AlCrN tool coatings sliding against Al-Si coated 22MnB5 steel exhibited very similar initial surface roughness ($1.45 \pm 0.15\,\mu$m for AlCrN 1 and $1.43 \pm 0.21\,\mu$m for AlCrN 2), but Figure 7 shows that the average specific wear rate of the AlCrN 2 coating is higher than the one of the AlCrN 1 coating, i.e., more material is transferred to the AlCrN 2 coated tool. It is either the stoichiometric composition of the PVD coating or the amount of a specific constituent available in a thicker PVD coating that influence this wear behaviour. Figure 7 shows that the material build-up on PVD coated tools containing aluminium is higher than for the CrWN coated tool. Merklein et al. [15] pointed out that, for monolayer PVD tool coatings, apart from the hardness, the stoichiometric composition of the coatings influences their wear behaviour. This is further emphasised by Rabinowicz [16], who considers metal pairs to be "metallurgically compatible" if their binary phase diagram indicates liquid miscibility and either complete solid solubility or solid solubility of one metal in the other at room temperature. This "metallurgical compatibility" leads to severe adhesion and then governs the tribological behaviour. However, Zum Gahr [17] stated that this model of mutual solubility (metallurgical compatibility) is not applicable to adhesion, friction, and wear as binary phase diagrams show the solubility in thermodynamic equilibrium. According to the author, mutual solubility only significantly contributes to friction and wear if the activation energy (e.g., temperature) for diffusion is exceeded (roughly 0.5 times the melting temperature) during sufficient time. It is clear that friction and wear are nonequilibrium processes. Though, when considering Rabinowicz' "compatibility chart", it can be observed that aluminium is "compatible" with most of the alloying elements used in steels. That means that the constituting elements of the investigated PVD coatings will all develop adhesive junctions with the Al-Si coating to a certain degree. Sánchez-López et al. [5] also mentioned that the tribological behaviour of CrAlN coatings was highly dependent on the nature of the counterface material and hence, when ductile materials such as Ti or Al alloys would be used as counter-surface, the adhesion of material from it would increase and the coefficient of friction would predominately be governed by the shear properties of the material transfer layer and the counter-surface. The current results clearly indicate that PVD coatings containing aluminium are less suitable to prevent the material transfer.

3.2.1. Behaviour of Al-Si Coated 22MnB5 Steel. Pelcastre et al. [18] described the phases present in the Al-Si coated 22MnB5 steel in its as-delivered state. The coating showed a considerable amount of voids before the material underwent the alloying procedure. Light optical micrographs of cross-sections of the alloyed Al-Si coating by Kondratiuk and Kuhn also revealed voids and high surface roughness or valleys [3]. These valleys have an effect on the tribological behaviour. It is clear that the type and concentration of defects in the Al-Si coating and its different constituents such as Fe-Al intermetallic compounds are important factors influencing the coating's mechanical properties and tribological performance. Pelcastre et al. [18] also mentioned that the friction and material transfer behaviours are affected by the phases in the Al-Si coating and that increased material transfer seen in some experiments was due to the presence of molten Al-Si coating or extremely soft phases. According to the authors, when $FeAl_2$ and Fe_2Al_5 have grown to the surface of the Al-Si coating on the 22MnB5 sheet steel during the alloying procedure, their high hardness increases wear of the counter surface due to more severe abrasion than without the intermetallic compounds present in the contact. Figure 8 depicts typical wear tracks observed on Al-Si coated 22MnB5 steel after sliding against different tool pins. It is derivable that, when the tool steel pins start to slide over the hot sheet strip, the highest asperities are sheared off due to the high local stresses occurring at asperity level. This shearing-off of surface asperities is observable on the Al-Si coated 22MnB5 sheet strip after contact with different tool materials in Figure 8. During this stage, a considerable amount of wear debris are generated and once formed, they will play an important role in the subsequent wear and friction mechanisms. These particles can be observed on the sheet strip surfaces. The surface valleys observed on the alloyed Al-Si coated 22MnB5 steel will entrap such debris generated during the wear process. Though, loose particles can also be reintegrated into material transfer layers or cause three-body abrasive wear on the tool steel surface. It is also evident that agglomeration and compaction of wear debris on the surface of the Al-Si coated sheet strip are present and influencing the wear behaviour. Considering the iron-aluminium binary phase diagram, Al-rich intermetallic compounds such as $FeAl_2$, Fe_2Al_5, and Fe_4Al_{13} were reported to exhibit complex crystal structures,

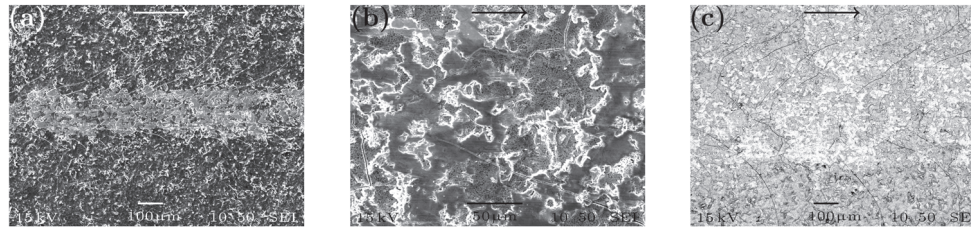

Figure 8: Scanning electron micrographs (a) in secondary electron mode of Al-Si coated 22MnB5 steel strip tested against uncoated tool steel, (b) in secondary mode of Al-Si coated 22MnB5 steel that slid against CrWN coated tool steel, and (c) in backscatter mode of Al-Si coated 22MnB5 steel strip tested against CrWN coated tool steel showing the cracking behaviour; Note that different magnifications were employed and that arrows indicate the sliding direction.

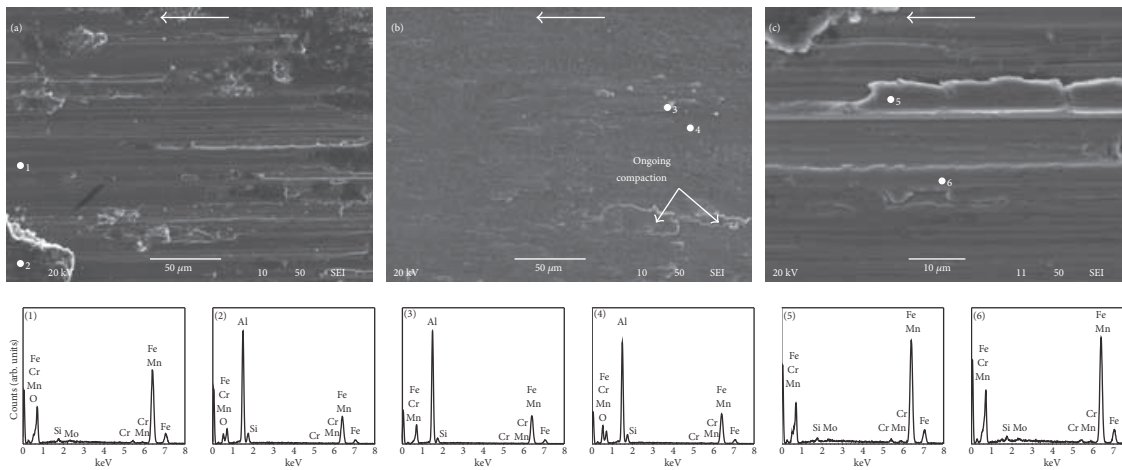

Figure 9: Scanning electron micrographs in secondary electron mode of (a) uncoated tool steel tested against Al-Si coated 22MnB5 steel and (b) on the load-bearing compacted debris layer and (c) the newly exposed tool steel surface in the contact; arrows indicate the sliding direction.

poor ductility, and low fracture toughness and consequently a brittle mechanical behaviour at low temperatures [19, 20]. Though, cracks, oriented at a 45° angle to the sliding direction in the wear track and that propagate into a perpendicular orientation to the sliding direction, indicate brittle fracture of the Al-Si coating due to high tangential stresses at the sliding interface.

3.2.2. Characteristics of Uncoated Tool Steel. Figure 9(a) reveals that the uncoated tool steel surface sliding against Al-Si coated 22MnB5 steel is primarily worn through adhesive wear with ploughing by either small particles seen as sharp grooves parallel to the sliding direction or larger material clusters with material transfer seen as thick more irregular grooves. Spectrum (1) in Figure 9 confirms that it is the tool steel material that is worn. It is further observable in Figure 9(a) that material adhering to the sheet surface got stuck in different ploughing tracks. There are two possible explanations for this behaviour. On one hand, waviness of the coating on the sheet surface results from the hot dipping process to coat the 22MnB5 steel and it is retained after austenitisation. Furthermore, small particles resulting from wear of the tool and sheet surfaces in contact can be agglomerated and compacted to larger material clusters (lumps) on the sheet surface. This has been termed as compaction galling. Compaction galling occurs when wear debris accumulates in surface valleys or surface defects and, as sliding progresses, provides sites for more entrapment of debris until compacts of the hard Fe-Al-Si intermetallics mixed together with oxidised debris from the tool start to form [13]. The large protuberances plough through the tool surface as the intermetallic phases formed in the coating during austenitisation are relatively harder. When the protuberance is trapped in the ploughing groove, it detaches from the sheet surface and remains in the groove on the tool surface as it is the tool that is moving. On the other hand, a protuberance might be pushed out of its ploughing groove as the contact evolves and small wear debris will then be entrapped in this groove and begin to accumulate until such a material cluster comes in contact with the counter-surface and further gets fragmented and compacted. Depending on the height of the protuberances on the sheet surface, the ploughing grooves and material ridges on the tool surface can grow up to several tenth of micrometres in size. When the material

detaches, the shear stress in the contact interface is reduced. Furthermore, at sites where mechanical interlocking occurs, debris will accumulate whilst sliding further progresses and lead to growing of this lump adhering to the tool surface. Such entrapped fragments of material also form obstacles on the tool surfaces for the counter-surface and any material in the interface. These entrapped fragments then increase the likelihood of localised mechanical interlocking. Thus, the conditions for formation and growth of adhesive junctions between the tool and the Al-Si coated 22MnB5 steel are enhanced.

The broken edge of a thicker material transfer layer that became load-bearing during subsequent sliding can also be observed in Figure 9(a). Spectrum (2) in Figure 9 taken on this transfer layer reveals that it mainly consisted of Fe and Al with some Si from the sheet coating material with an approximate composition of $FeAl_2$ that is partially oxidised. Furthermore, when examining the edge of the load-bearing material transfer layer, it is obvious that this layer is composed of agglomerated and compacted debris. Van Alboom et al. [21] pointed out that an integer stoichiometry of intermetallic θ and η-layers (seen as equivalent to Fe_4Al_{13} and Fe_2Al_{5+x}, respectively) formed at the surface of hot-dip aluminised steel suggested a well-defined composition. The authors further stated that Fe_2Al_{5+x} exhibited a partially disordered crystal structure as some Al atomic sites only were partially occupied. This means that some Al atomic sites in the crystal lattice are vacant and the intermetallic compounds are probably chemically active. Hence, these Fe-Al intermetallic compounds possess a higher tendency to adhere to Fe that is available on the tool steel surface. This can be an explanation for the formation of adhesive metallic junctions between the uncoated tool steel and the intermetallic phases in the Al-Si sheet coating. The growth of adhesive oxide junctions between the tool steel and the Al-Si coating material on the 22MnB5 sheet steel might be motivated in a similar way as the surrounding environment contains oxygen. This can also be enhanced owing to the high test temperature of 750°C.

Additionally, the built-up of compacted oxide patches is a function of the number of sliding passes over a given point on the surface rather than a function of the actual sliding time according to Stott and Wood [10]. In hot strip drawing tests, a given spot on the tool is exposed to several consecutive contacts with a fresh counter surface. This means that isolated patches with some load-carrying capacity can be formed and stick to the rubbing surfaces as, for example. depicted in Figure 9. Stott and Wood further explained [10] that the very smooth surface of load-bearing areas was due to comminution of oxide into very fine particles. The wear rate is then comparably small as oxidised wear debris either gets reintegrated into the adhered material on the surface from which it originated or is transferred and compacted into the opposing surface. These islands can also reduce friction to some extent as both contributions of ploughing and adhesion to friction become limited. This behaviour occurs regardless of the surface conditions of the 22MnB5 steel (uncoated or Al-Si coated). Figure 9(b) shows the surface of a load-bearing material transfer layer. It can be seen that newly generated wear particles from the coating with an approximate composition of $FeAl_2$ that start to oxidise are on top of the oxidised material transfer layer. Moreover, it can be noticed that another spot on the load-bearing transfer layer was undergoing compaction galling. However, it is also evident that the material transfer layer is beginning to mechanically fail as transversal cracks start to develop that are seen as dark irregular lines perpendicular to the sliding direction. Figure 9(c) indicates that the uncoated tool steel sliding against Al-Si coated 22MnB5 steel at 750°C is also severely worn through adhesive wear and ploughing. When ploughing occurs, tool steel material is pushed over the edges of the ploughing groove, resulting in excess material ridges. During subsequent sliding of new sheet material over the tool surface, these ridges can be detached resulting in formation of wear debris. Such debris will then play an important role in the outlined tribological mechanisms.

3.2.3. Characteristics of PVD Coated Tool Steel. Figure 10(a) shows how wear debris starts to accumulate just outside the wear track at the entrance of the contact zone on a TiAlN coated tool steel specimen that slid against Al-Si coated 22MnB5 steel. It should be noted that these wear particles still adhered to the surfaces even though the pin specimens were cleaned in an ultrasonic bath in heptane and ethanol for a total of 10 minutes, which indicates a strong adhesion between the PVD coating and the transferred material. In the case of uncoated tool steel, the affinity of the intermetallic compounds in the transferred material is towards the constituents on the tool steel surface. In the case of PVD coated tools, the intermetallic compounds seem to be foremost attracted to PVD coatings containing Al, but material transfer also occurs on the PVD coating without Al. Further investigations are required to fully comprehend this behaviour. The fine particles seen in Figure 10(a) could get trapped in surface imperfections like dimples and scratches and further agglomerate new sheet material at such spots in consecutive passes. Pelcastre et al. [13] also found that a high chemical affinity between the Al-Si coated 22MnB5 steel and the PVD coating constituents on the tool steel pins appeared to be the main driving force for galling. According to the authors, the influence of the surface topography was less significant than for uncoated tool steel material. Figure 10(b) shows that wear debris also accumulates just outside the wear track at the exit of the contact zone on another TiAlN coated tool steel specimen after sliding against Al-Si coated 22MnB5 steel. It can be seen that an initial thin film of transferred material, seen as a darker area, has formed around a groove and starts to form a continuous layer partially covering the groove. This strengthens the hypothesis of initial direct adhesion. It can further be seen that particle agglomeration has started at small dimples close to the larger transferred material cluster. Figure 10(c) depicts the scanning electron micrograph at 60° tilting angle in secondary electron mode of the AlCrN 1 coating after sliding against Al-Si coated 22MnB5 steel. It can be seen that the transfer layer has a structure which is formed through compaction and possibly partial sintering of wear debris. The layer has considerable porosity since the contact pressures are only moderate or low,

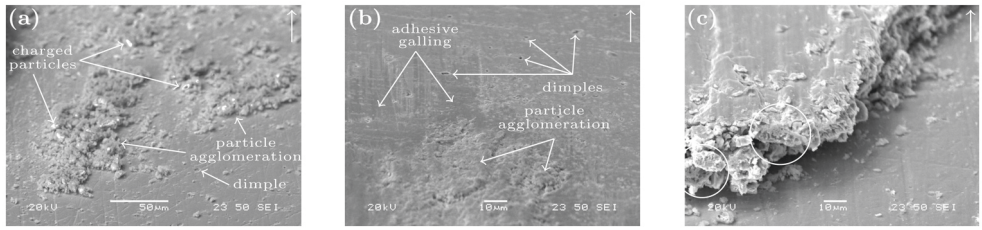

(a) (b) (c)

Figure 10: Scanning electron micrographs at 60° tilting angle in secondary mode of (a) the entrance to the contact (converging gap) on one and (b) the exit of the contact (diverging gap) on another TiAlN coated tool steel pin and (c) of the edge of the material transfer layer on an AlCrN 1 coated tool steel pin after sliding against Al-Si coated 22MnB5 steel; arrows indicate the sliding direction.

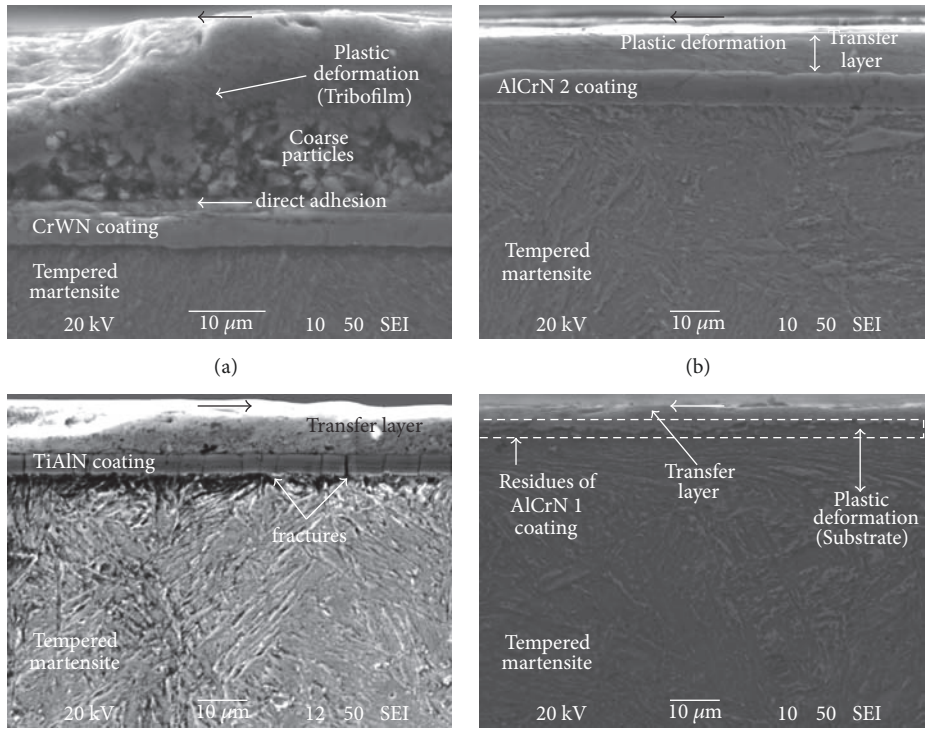

Figure 11: Scanning electron micrographs in secondary electron mode of longitudinal sections of (a) CrWN coated tool close to the entrance to the contact, (b) AlCrN 2 coated tool in the front half of the contact, (c) TiAlN coated tool in the rear half of the contact and (d) AlCrN 1 coated tool close to the exit of the contact after tribological tests; arrows indicate the sliding direction.

which innately has an effect on their mechanical strength. Even though the top surface is very smooth and should contribute to a reduced coefficient of friction, the incomplete sintering of agglomerated and compacted wear particles will be detrimental to the load-bearing capacity of the material transfer patches. When new sheet coating material comes in contact, cracks will begin to appear in the porous transfer film at much lower shear stresses than the shear strength of the constituting, bulk phases that were transferred. Once initiated, such cracks will propagate easily through the porous transfer layer leading mainly to brittle fracture due to the presence of hard Fe-Al intermetallic compounds. Consequently, this will result in generation of wear debris that can further form compacted transfer layers or these particles can locally increase the contact pressure, similar to an indenter, so that the tool steel substrate will plastically deform underneath the PVD coating resulting in its mechanical rupture.

Figure 11 shows longitudinal sections of the transferred material on the PVD coated tool steel pins for illustrative purposes. It is worth noting that all PVD coatings showed the same wear characteristics in the longitudinal sections. In Figure 11(a), it can be seen that the transferred material on the CrWN coated tool steel after sliding against Al-Si coated 22MnB5 steel consists of particles of different sizes that are mixed and sintered together. The transfer layer is densely packed at the top surface and even plastically deformed and

oriented into the sliding direction. In the middle, the material transfer layer is composed of debris that is coarser and not fully compacted. As the PVD coating has not completely failed in this case, it can be assumed that the transfer layer mainly consists of Fe-Al intermetallic phases originating from the Al-Si coating material on the counter surface. Below the coarse layer, a thin continuous layer of about 1 micrometre thickness can be seen. This is believed to form through direct adhesion. The densely packed top layer was built up due to entrapment and blocking of debris in the converging gap of the interface. The coarser layer is debris that was transported on top of the dense layer and may even be particles that broke loose from the dense layer built up in front of the contact zone. In Figure 11(b), it can be seen that a dense material transfer layer of approximately 10 micrometres is adhering to the AlCrN 2 coated tool pin surface after sliding against Al-Si coated 22MnB5 steel. This dense layer also shows that its microstructure is elongated into the sliding direction as a result of the tangential stresses. Furthermore, the PVD coating shows cracks that either initiate from the tribolayer-coating interface or from the tool steel-coating interface. However, these cracks do not propagate through the PVD coating right away but deviate into a direction parallel to the interfaces. This behaviour can even be seen in Figure 11(a) for the CrWN coated tool pin at the entrance to the contact. It is known that interstitial nitrides commonly exhibit a ductile-to-brittle transition temperature at about 800°C [22]. Therefore, a brittle mechanical behaviour of the PVD coating at a test temperature of 750°C is anticipated. The reason for the deviation of cracks are the normal and tangential stresses which are more severe than on a flat tool surface due to the geometric shape of the tool pins. Moreover, the directions and magnitudes of the normal and tangential fractions of the stresses in the contact vary throughout the interface plane and the depth into the material. Then, the stress concentration profiles will vary during contact as the material transfer layer continuously builds up and breaks down. This could be an explanation for the cracking behaviour observed for the PVD coated tool steels. Figure 11(c) illustrates the brittle fracture of the PVD coating. It is believed that as the transfer layer is built up, the normal pressure onto the pin specimen surfaces increases. Upon reaching a threshold value, the tool steel substrate, as it is softer and ductile, is unable to mechanically support the much harder PVD coating. Hence, the PVD coating fractures from the coating-tool steel interface due to tensile stresses. Heat transfer from the hot sheet strip might also enhance this behaviour through thermal softening of the tool steel substrate. Towards the exit of the contact zone, seen in Figure 11(d), a 5-micrometre thick dense material transfer layer can be observed on the AlCrN 1 coated tool pin surface after sliding against Al-Si coated 22MnB5 steel. The tool steel microstructure below the PVD coating is highly deformed and oriented into the sliding direction. This orientation of the tool steel microstructure is observed in all cases where the PVD coating has been fractured or been partially removed. Such plastic deformation and orientation of the tool steel microstructure into the sliding direction was also observed by Boher et al. [23]. This occurs owing to contributions of normal and tangential stresses due to the curvature of the tool pin. The Cr element map corresponding to the scanning electron micrograph in Figure 11(d) revealed that the AlCrN 1 coating at the transfer layer-tool steel interface had not been entirely removed. These four different zones of varying wear severity appeared on all PVD coated tool steels that slid against Al-Si coated 22MnB5 steel.

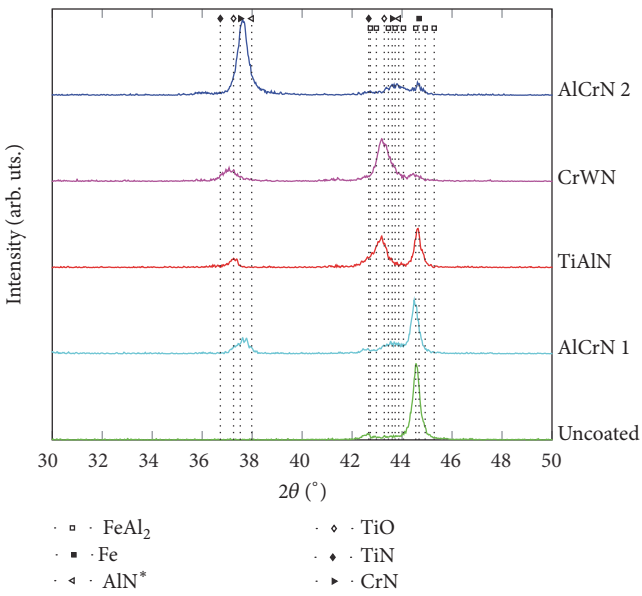

FIGURE 12: X-ray diffractograms of the uncoated and PVD coated tool pin surfaces after sliding against Al-Si coated 22MnB5 steel. *Diffraction angle for cubic AlN taken from [25].

3.2.4. X-Ray Diffraction. The layered microstructure of the Al-Si coated 22MnB5 steel that is obtained after austenitisation of the sheet material has been characterised [3, 18, 23, 24]. This layered morphology mainly consists of binary and ternary iron, aluminium, and silicon intermetallic phases such as $FeAl_2$, Fe_2Al_5, Fe_2Al_2Si, and $Fe_2Al_{7-8}Si$. Furthermore, microstructural analysis has revealed that the binary iron-aluminium phases $FeAl_2$ and Fe_2Al_5 constitute the largest volume of the Al-Si coating. Therefore, it is believed that either $FeAl_2$, Fe_2Al_5, or both are present in the material transfer layer on the tool specimen surfaces after tribological interaction. To confirm this, X-ray diffractometry using Cu-K_α radiation was performed on uncoated and PVD coated tool specimens that slid against Al-Si coated 22MnB5 steel. The motivation for this analysis is the identification of the phases present in the transferred material layer on the tool surfaces. This is done in view of developing more suitable methods to prevent material transfer from the work piece to the forming tool. Figure 12 shows the most interesting angular range of the X-ray diffractograms for the analysed pin specimen surfaces after sliding against Al-Si coated 22MnB5 steel. In the case of PVD coated tool steel, the identified underlying base coatings exhibit a face-centred cubic ($Fm\bar{3}m$ space group 225) crystalline structure with lattice parameters of 4.235 Å for TiN and 4.148 Å for CrN. Iron peaks in the diffractograms originate from the quenched and tempered

tool steel substrate, but these peaks are shifted and/or broadened as the substrate material is an alloyed tool steel rather than pure iron. The alloying elements will also influence the peak intensity. In all X-ray diffractograms, smaller peaks can be observed at diffraction angles between 42.0° and 43.0°. These are identified as originating from the intermetallic compound $FeAl_2$. This means that the transferred material is to some extent metallic in nature despite the high temperature contact. However, it should be kept in mind that the material transfer layer exhibits a highly deformed microstructure. The enduring mechanical contact and relative motion between the materials subjects the surface and subsurface areas to high plastic stress and creates an orientation into the sliding direction in the subsurface crystallites, as was observed in Figure 11. This could be the reason why some peaks in the diffractograms might be less intense or even missing. It is known that, in a θ-2θ scan, peaks will shift to lower angles for compressive stresses and to higher angles for tensile stresses. Moreover, in a strained sample, peak shifts will be greater at higher angles than at lower angles. Van Alboom et al. [21] pointed out that a fair amount of confusion existed regarding the compositions of the intermetallic layers formed at the surface of hot-dip aluminised steel. They reported that these phases corresponded to Fe_4Al_{13} and Fe_2Al_{5+x} rather than $FeAl_3$ and Fe_2Al_5. When further considering the Fe-Al binary phase diagram, it can be observed that the intermetallic phases $FeAl_2$ and Fe_2Al_5 do not possess an exactly defined stoichiometric composition, which means that their composition can vary to a certain degree. To the best of our knowledge, information about the crystal structures of Fe-Al intermetallic compound oxides is not available in the open literature. Hence, unambiguous identification of phases is challenging. However, Venema et al. [26] also identified through X-Ray diffraction that dust on the tool mainly contained intermetallic compounds such as Fe_2Al_5 and FeAl originating from the sheet coating as well as ferrite that could stem either from the tool or the sheet material. In the present work, peaks of pure aluminium were not found, even though pure aluminium has been reported to be sometimes present in the sheet coating and consequently could be suspected in the transfer film [18]. A possible reason for this could be that the relative volume of pure aluminium is small due to its high reactivity and oxygen affinity, so that the quantity is beyond the detection limit of the instrument.

4. Conclusions

In this work, the tribological behaviour of uncoated and four different PVD coated tool steels was investigated when sliding against uncoated and Al-Si coated 22MnB5 steel at a temperature of 750°C in an experimental set-up simulating press hardening contact conditions.

It was found that uncoated tool steel exhibited the lowest coefficient of friction when sliding against uncoated 22MnB5 steel. This was attributed to a faster reduction in contact pressure as uncoated tool steel is softer and will be subjected to more deformation and material removal. CrWN coated tool steel initially showed low coefficient of friction but it increased with increasing sliding distance. TiAlN coated tool steel and two AlCrN coatings showed unstable friction coefficients. A clear difference in frictional behaviour due to plasma nitriding of AlCrN 1 coated tool steel was not observed when comparing to AlCrN 2 coated tool steel without plasma nitriding. PVD coated tools exhibited higher coefficients of friction due to a larger contribution from ploughing friction in the counter-surface. Irregular features on the worn surfaces of uncoated tool steel that slid against uncoated 22MnB5 steel confirmed an adhesive wear behaviour. As oxide was removed by the sliding action, considerable metal-to-metal contact occurred which resulted in substantial material removal. The specific wear rates of PVD coated tools were reduced in comparison to uncoated tool steel sliding against uncoated 22MnB5 steel. The main mechanism for the occurrence of adhesion was initial direct adhesion followed by agglomeration and compaction of generated debris mainly consisting of Fe and O.

It was further confirmed that uncoated and PVD coated tools exhibited indistinguishable friction behaviour during sliding against Al-Si coated 22MnB5 steel. This indicates that friction is governed by the Al-Si coating on the 22MnB5 sheet material whereas the tool coating does not influence the friction behaviour significantly. There is evidence that the stoichiometric composition of the PVD coating influences the wear behaviour in the case of Al-Si coated 22MnB5 steel as the material build-up on PVD coated tools containing aluminium is higher than for a CrWN coated tool without aluminium. The specific wear rates of PVD coated tools were reduced in comparison to uncoated tool steel in the case of Al-Si coated 22MnB5 steel. X-ray diffractometry of the material transfer layer on all tools confirmed the existence of Fe-Al intermetallic compounds in this layer although it is highly strained and partially oxidised.

In general, after wear particles are generated, material transfer initiates with the agglomeration of debris at surface imperfections such as directly adhered particles, protrusions or dimples, fractures or even abrasive marks. Further fragmentation, compaction, and oxidation of these agglomerates lead to adhered material clusters that plough through the counter-surface. Such material clusters get mechanically interlocked in ploughing grooves and at adhering agglomerates, where further generated debris results in considerable material build-up. The material transfer layer can separate the surfaces and carry the load to some extent. However, it is mechanically fragile and breaks and the process of material transfer layer formation on tools tested against Al-Si coated 22MnB5 steel repeats itself. In brief, all cases exhibit some form of agglomeration, fragmentation, compaction, and sintering of wear particles, whether it is uncoated or PVD coated tool steel sliding against uncoated or Al-Si coated 22MnB5 steel. Although the PVD coated tool steels considerably reduced the specific wear rate, yet their overall performance is unsatisfactory.

Data Availability

The data used to support the findings of this study are available from the corresponding author upon request.

Conflicts of Interest

The authors declare that they have no conflicts of interest.

Acknowledgments

This work was in part presented at the International Tribology Conference (ITC) 2015 in Tokyo, Japan. The authors would like to express their gratitude to the organisers for the opportunity to disseminate their research. The authors would also like to thank Oerlikon Balzers Sandvik Coating AB and Ionbond Sweden AB for providing coatings for this investigation and for their keen interest in this research. This work was funded by the Swedish Governmental Agency for Innovation Systems, Vinnova, and the programme FFI, Sustainable Production Technology [grant number 2010-02851]. The authors wish to express their gratitude for the support.

References

[1] J. Hardell and B. Prakash, "Tribological performance of surface engineered tool steel at elevated temperatures," *International Journal of Refractory Metals and Hard Materials*, vol. 28, no. 1, pp. 106–114, 2010.

[2] M. Wieland and M. Merklein, "Wear behavior of uncoated and coated tools under complex loading conditions," *Tribology in Industry*, vol. 34, no. 1, pp. 11–17, 2012.

[3] J. Kondratiuk and P. Kuhn, "Tribological investigation on friction and wear behaviour of coatings for hot sheet metal forming," *Wear*, vol. 270, no. 11-12, pp. 839–849, 2011.

[4] R. Neugebauer, F. Schieck, S. Polster et al., "Press hardening - An innovative and challenging technology," *Archives of Civil and Mechanical Engineering*, vol. 12, no. 2, pp. 113–118, 2012.

[5] J. C. Sánchez-López, A. Contreras, S. Domínguez-Meister, A. García-Luis, and M. Brizuela, "Tribological behaviour at high temperature of hard CrAlN coatings doped with Y or Zr," *Thin Solid Films*, vol. 550, pp. 413–420, 2014.

[6] S. Mozgovoy, J. Hardell, L. Deng, M. Oldenburg, and B. Prakash, "Tribological behavior of tool steel under press hardening conditions using simulative tests," *Journal of Tribology*, vol. 140, no. 1, pp. 011606–1–011606–11, 2018.

[7] F. Stein, G. Sauthoff, and M. Palm, "Phases and phase equilibria in the Fe-Al-Zr system," *Zeitschrift fuer Metallkunde*, vol. 95, no. 6, pp. 469–485, 2004.

[8] J. F. Archard and W. Hirst, "The wear of metals under unlubricated conditions," in *Proceedings of the Royal Society of London. Series A. Mathematical and Physical Sciences*, vol. 236, pp. 397–410, 1956.

[9] J. F. Archard, "Contact and rubbing of flat surfaces," *Journal of Applied Physics*, vol. 24, no. 8, pp. 981–988, 1953.

[10] F. H. Stott and G. C. Wood, "The influence of oxides on the friction and wear of alloys," *Tribology International*, vol. 11, no. 4, pp. 211–218, 1978.

[11] L. Deng, S. Mozgovoy, J. Hardell, B. Prakash, and M. Oldenburg, "Development of a tribological test programme based on press hardening simulations," *Tribology Letters*, vol. 65, no. 2, pp. 43–1–43–11, 2017.

[12] S. Mozgovoy, J. Hardell, L. Deng, M. Oldenburg, and B. Prakash, "Effect of temperature on friction and wear of prehardened tool steel during sliding against 22MnB5 steel," *Tribology - Materials, Surfaces and Interfaces*, vol. 8, no. 2, pp. 65–73, 2014.

[13] L. Pelcastre, J. Hardell, and B. Prakash, "Galling mechanisms during interaction of tool steel and Al-Si coated ultra-high strength steel at elevated temperature," *Tribology International*, vol. 67, pp. 263–271, 2013.

[14] J. Hardell, B. Prakash, and K. Steinhoff, "High temperature tribological studies on surface engineered tool steel and high strength boron steel," *Steel Research International*, vol. 80, no. 9, pp. 665–670, 2009.

[15] M. Merklein, T. Schrader, and U. Engel, "Wear behavior of PVD-coatings," *Tribology in Industry*, vol. 34, no. 2, pp. 51–56, 2012.

[16] E. Rabinowicz, *Friction and Wear of Materials*, John Wiley & Sons, Inc, NY, NY, USA, 2nd edition, 1995.

[17] K.-H. Zum Gahr, *Microstructure and Wear of Materials*, K.-H. Zum Gahr, Ed., vol. 10 of *Tribology Series*, Elsevier Science, 1987.

[18] L. Pelcastre, J. Hardell, A. Rolland, and B. Prakash, "Influence of microstructural evolution of Al-Si coated UHSS on its tribological behaviour against tool steel at elevated temperatures," *Journal of Materials Processing Technology*, vol. 228, pp. 117–124, 2016.

[19] M. Zamanzade, A. Barnoush, and C. Motz, "A review on the properties of iron aluminide intermetallics," *Crystals*, vol. 6, no. 1, pp. 10–39, 2016.

[20] P. Matysik, S. Józwiak, and T. Czujko, "Characterization of low-symmetry structures from phase equilibrium of Fe-Al system-microstructures and mechanical properties," *Materials*, vol. 8, no. 3, pp. 914–931, 2015.

[21] A. Van Alboom, B. Lemmens, B. Breitbach, E. De Grave, S. Cottenier, and K. Verbeken, "Multi-method identification and characterization of the intermetallic surface layers of hot-dip Al-coated steel: FeAl3 or Fe4Al13 and Fe2Al5 or Fe2Al5+x," *Surface and Coatings Technology*, vol. 324, pp. 419–428, 2017.

[22] H. O. Pierson, *Handbook of Refractory Carbides and Nitrides: Properties, Characteristics, Processing, and Applications*, Noyes Publications/William Andrew Publishing, Norwich, NY, 1996.

[23] C. Boher, S. Le Roux, L. Penazzi, and C. Dessain, "Experimental investigation of the tribological behavior and wear mechanisms of tool steel grades in hot stamping of a high-strength boron steel," *Wear*, vol. 294-295, pp. 286–295, 2012.

[24] A. Ghiotti, S. Bruschi, and F. Borsetto, "Tribological characteristics of high strength steel sheets under hot stamping conditions," *Journal of Materials Processing Technology*, vol. 211, no. 11, pp. 1694–1700, 2011.

[25] K. Bobzin, N. Bagcivan, M. Ewering, and R. H. Brugnara, "Vanadium alloyed PVD CrAlN coatings for friction reduction in metal forming applications," *Tribology in Industry*, vol. 34, no. 2, pp. 101–107, 2012.

[26] J. Venema, D. T. A. Matthews, J. Hazrati, J. Wörmann, and A. H. van den Boogaard, "Friction and wear mechanisms during hot stamping of AlSi coated press hardening steel," *Wear*, vol. 380-381, pp. 137–145, 2017.